

Vibrational evidence for a percolative behavior in $\text{Zn}_{1-x}\text{Be}_x\text{Se}$

O. Pagès* and M. Ajjoun

Institut de Physique, 1 Boulevard Arago, 57078 Metz, France

D. Bormann

Laboratoire de Physico-Chimie des Interfaces et Applications, Rue J. Souvraz, 62037 Lens, France

C. Chauvet, E. Tournié, and J. P. Faurie

Centre de Recherche sur l'Hétéroépitaxie et ses Applications, Rue B. Gregory, 06560 Valbonne, France

(Received 21 February 2001; revised manuscript received 20 June 2001; published 28 December 2001)

We present an atypical multimode behavior in the Raman spectra recorded with $\text{Zn}_{1-x}\text{Be}_x\text{Se}$, which belongs to the new class of ternary semiconductor alloys made of materials with highly contrasted bond stiffness. We observe the activation of a strong extra BeSe-like optical mode for x between the percolation thresholds of the Be-Se and Zn-Se bonds. This extra mode is attributed to Be-Se bonds within the quasicontinuous Be-rich hardlike cluster that forms above the percolation threshold. Our observations can be quantitatively explained in terms of a generalized version of the standard modified-random-element-isodisplacement model.

DOI: 10.1103/PhysRevB.65.035213

PACS number(s): 78.30.Fs, 63.20.Pw, 64.60.Ak

I. INTRODUCTION

In semiconductor alloys $A_{1-x}B_xC$ random atomic substitution brings major topological changes at the percolation thresholds of $A-C$ and $B-C$ bonds. These are defined as the critical compositions associated with the first formation of pseudocontinuous wall-to-wall chains of the corresponding bonds, and were identified at $x = x_{B-C} \sim 0.19$ and $x = x_{A-C} \sim 0.81$ in zinc-blende systems.¹ In usual alloys these major changes do not go with anomalies for the current physical properties, which exhibit most of the time a nearly linear dependence on the composition x . This is because parent materials are chosen similar in nature, in order to avoid structural phase transitions or direct-to-indirect band-gap crossovers.¹ However, it is necessary to mention that percolation concepts were introduced to analyze the advanced characterization of phonon^{2,3} and carrier transport⁴ in AlGaAs.

Recently the attention turned towards the new attractive class of zinc-blende ternary alloys made from binaries with highly contrasted mechanical properties, and deviations from this simple picture were predicted. In particular, in $\text{GaAs}_{1-x}\text{N}_x$ Bellaïche, Wei, and Zunger expect striking bond-length anomalies at the bond-percolation thresholds.¹ They also found that the band-gap bowing would become unusually large and composition dependent. We are not aware of any prediction/observation of specific vibrational properties in mixed compounds with contrasted bond stiffness. Nevertheless, latter class of alloys opens the way for the observation of percolative effects by vibrational spectroscopies since these techniques address directly the force constant of the bonding, which is extremely sensitive to the mechanical properties of the host matrix.

Mixed crystal ZnSe-BeSe is another system with a sharp contrast in mechanical properties of the two constituents. Vérié⁵ has predicted a highly covalent bonding for BeSe, which finds its expression in a reduced lattice parameter of 5.037 Å and a remarkably high reduced shear modulus C_s^* of

0.478. Corresponding values for ZnSe are, respectively, 5.669 Å and 0.277.⁶ C_s^* is a pertinent marker for lattice stiffness as it is primarily determined by the noncentral force constant, denoted by β in the Martin's notation, which can be simply interpreted as the bond-bending force constant.⁶ For comparison, we notice that in other mixed compounds with a lattice mismatch similar to system ZnSe-BeSe (9%), such as InAs-GaAs (7%) for III-V materials and ZnS-ZnTe (9%) for II-VI's, C_s^* differs by less than 25%,⁶ while it almost doubles between ZnSe and BeSe. The main aim of Be incorporation in ZnSe is precisely to strengthen latter softlike highly ionic lattice so as to reduce defect propagation and rehabilitate II-VI materials for the design of blue-UV optoelectronic systems.^{7,8}

The zone-center ($q \sim 0$) longitudinal optical (LO) and transverse optical (TO) phonons of BeSe and the alloy $\text{Zn}_{1-x}\text{Be}_x\text{Se}$ were recently identified in earlier infrared and Raman analysis.⁹⁻¹² Most of the Raman spectra were recorded with the (LO allowed, TO forbidden) backscattering geometry.^{9,11} At first sight the alloy shows a two-mode behavior, as expected from the modified-random-element-isodisplacement (MREI) model.¹³ This typical behavior is indeed observed in similarly mismatched alloys ZnS-ZnTe (Ref. 14) and InAs-GaAs.¹⁵ However, out of the dilute limits ZnBeSe exhibits unexpectedly an additional mode, on top of the nominal MREI ones.^{10,11} Only little attention was awarded to this mode in previous studies. At the present stage, it appears that the extra mode does not result from structural disorder since high-crystalline quality is evidenced at any x by x-ray diffraction, nor from symmetry breaking due to lattice distortion¹⁶ since it obeys the standard $q \sim 0$ selection rules.¹¹ Besides it depicts an intrinsic feature since it occurs in epitaxial layers¹¹ as well as in bulk-mixed crystals.¹⁰ It was first assigned from Raman analysis as the ZnSe-like 2TO ($2\text{TO}_{\text{Zn-Se}}$) mode,¹⁰ but infrared measurements eventually showed that it split in a (TO,LO) doublet related to Be-Se bonds.¹¹

In this work, we present further analysis of the Raman

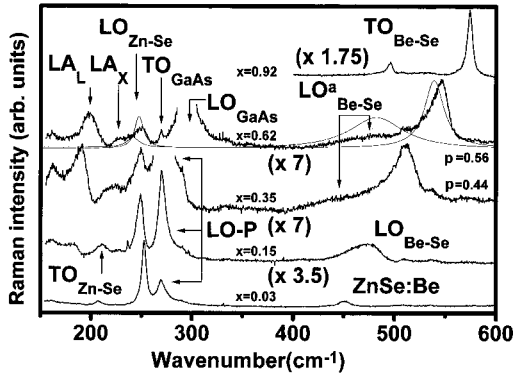


FIG. 1. Raman spectra for $\text{Zn}_{1-x}\text{Be}_x\text{Se}/\text{GaAs}$ in backscattering geometry along the $[001]$ growth axis. Label “a” refers to the “additional” LO branch. An example of two-mode LO simulations (see text) is shown by thin lines ($x=0.62$). The calculated ZnSe-like additional LO mode emerges at higher frequency than the “nominal” one. When relevant the p values corresponding to the best agreement are indicated.

spectra for this alloy throughout the whole composition range by using both LO- and TO-allowed scattering geometries, in order to get an insight on each component of the extra doublet. We find that the extra BeSe-like mode results from a specific percolative context that takes place only in alloys with highly contrasted bond stiffness.

After a brief description of the experimental details in Sec. II, we present our experimental results in details in Sec. III. Section IV contains our analysis of the Raman spectra in the context of the bond-percolation phenomena. Conclusions are summarized in Sec. V.

II. EXPERIMENT

We use $\sim 1\text{-}\mu\text{m}$ -thick $\text{Zn}_{1-x}\text{Be}_x\text{Se}$ layers covering the whole composition range, deposited by molecular-beam epitaxy on (001) GaAs. Unpolarized Raman spectra were recorded at room temperature, with the Dilor-microprobe setup, in the backscattering geometry, under standard illumination, with the 514.5-nm radiation from an Ar^+ laser as the exciting source. The excitation-detection direction was along the $[001]$ growth or $[110]$ edge crystal axis. In the first geometry LO modes are allowed and TO modes are forbidden; the situation is reversed in the second geometry. By using a green excitation the samples are transparent/absorbinglike so that the spectra recorded along the growth axis bring the responses from both the whole of the layer and the near-interfacial substrate. $\text{Zn}_{1-x}\text{Be}_x\text{Se}$ responses recorded along the edge axis refer to similar scattering volumes although the microprobe overlaps into GaAs in some cases, and can be directly compared in a first approximation.

III. EXPERIMENTAL RESULTS

Representative spectra obtained along the growth and edge axis are reported in Figs. 1 and 2, respectively. Concerning the substrate side, we just mention that the longitudinal optical response corresponds either to the LO mode, at

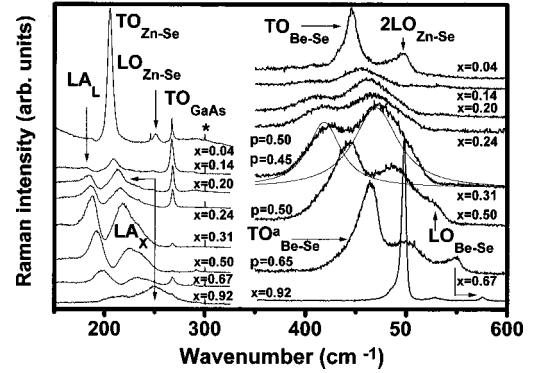


FIG. 2. Raman spectra for $\text{Zn}_{1-x}\text{Be}_x\text{Se}/\text{GaAs}$ in backscattering geometry along the $[110]$ edge axis. The high-frequency side of the spectra corresponding to $x \leq 0.67$ ($x=0.92$) is multiplied by 5 (divided by 20). Label “a” refers to the “additional” TO branch. An example of two-mode TO simulations (see text) is shown by thin lines ($x=0.31$). When relevant the p values corresponding to the best agreement are indicated. The star indicates a parasitical laser line.

292.3 cm^{-1} , or to a TO_{GaAs} -like (268 cm^{-1}) LO phonon-plasmon (LO-P) coupled mode involved with a hole gas.¹²

We first comment on the low-frequency signal from $\text{Zn}_{1-x}\text{Be}_x\text{Se}$. A well-known consequence of the lack of translational symmetry in a mixed crystal is the activation of broad features that mirror the one-phonon state density and correspond usually to zone-edge modes.¹⁷ This is evidenced here by the presence of the structures labeled LA_L and LA_X , which we assign as the longitudinal-acoustical bands at edges L and X .¹⁸ We underline that each LA band exhibits a single-mode behavior and slides between the corresponding binary frequencies, identified as $166\text{--}220\text{ cm}^{-1}$ for LA_L and $194\text{--}246\text{ cm}^{-1}$ for LA_X .¹⁸ The lower frequencies correspond to ZnSe and the higher ones to BeSe. Slight deviations from linearity may be attributed to line shape distortions of the LA continua due to Fano-like interferences¹⁹ with the discrete $q \sim 0$ TO_{ZnSe} mode that emerges around 220 cm^{-1} .^{9–12} This is suggested by the characteristic antiresonance that shows up within the overlapping energy range.¹² The key information here is that in both geometries the LA bands show extraordinary strength within the percolation regime ($x_{\text{BeSe}} < x < x_{\text{ZnSe}}$), with a maximum contribution at $x \sim 0.5$.

We consider now the $q \sim 0$ signal. As already mentioned most of the Raman spectra available in the literature refer to the LO symmetry, and are similar to those reported in Fig. 1. At first sight ZnBeSe seems to obey a typical MREI-like two-mode behavior, referred below as the “nominal” behavior. The ZnSe-like component, labeled LO_{ZnSe} , is located within the optical band of ZnSe, i.e., $206\text{--}253\text{ cm}^{-1}$, while the BeSe-like one, labeled LO_{BeSe} , shifts progressively between the local mode of Be in ZnSe at 445 cm^{-1} , labeled ZnSe:Be and the LO_{BeSe} mode at 578 cm^{-1} .^{9,12} We also notice that there is clear evidence of an additional mode, shown as $\text{LO}_{\text{BeSe}}^a$. This mode emerges only in the intermediate composition range, in the form of a broad and weak shoulder located on the low-frequency side of the nominal

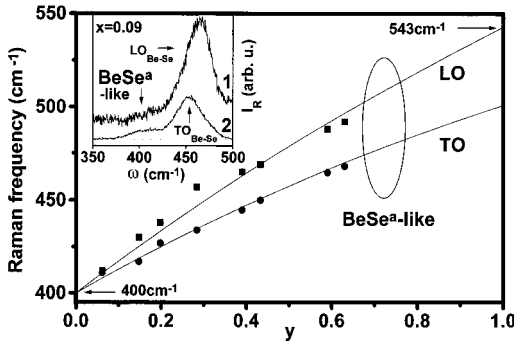


FIG. 3. Compositional dependencies of the additional $\text{TO}_{\text{Be-Se}}$ (circles) and $\text{LO}_{\text{Be-Se}}$ (squares) branches. Full lines indicate MREI predictions (see text) by using the specific end values indicated by the arrows. The additional mode observed at $x=0.09$ in the LO-allowed (1) and TO-allowed (2) geometries is shown in the inset. “ I_R ” and “ ω ” are condensed notations for Raman intensity and frequency respectively.

$\text{LO}_{\text{Be-Se}}$ mode. Its relatively small strength might explain why it attracted so little attention in the previous studies.¹¹

This additional mode appears strongly in the new data related to the TO symmetry, reported in Fig. 2. The Raman signal in the $400\text{--}600\text{ cm}^{-1}$ range can be divided into two contributions with similar intensities, so that the true bimodal character of the BeSe-like response becomes indisputable. The higher frequency mode corresponds to the nominal TO vibration and is labeled $\text{TO}_{\text{Be-Se}}$, while the additional mode appears on the lower frequency side, and is labeled $\text{TO}_{\text{Be-Se}}^a$. This multimode behavior is atypical since the extra mode is activated within the percolation regime only. Near $x \sim x_{\text{Be-Se}}$, we have investigated several samples with small changes in composition (refer to Fig. 2) and it is striking that $x_{\text{Be-Se}}$ corresponds indeed closely to the first clear emergence of the extra TO mode. Unfortunately, we did not have similar composition variation around $x_{\text{Zn-Se}}$. However, other work¹¹ has pointed out that the additional doublet can actually be observed up to $x=0.8$, corresponding to latter limit. For our part, we observe the $\text{TO}_{\text{Be-Se}}^a$ mode up to the highest Be content that we have within the percolation range, i.e., $x \sim 0.7$ (refer to Figs. 2 and 3), while it disappears at our first composition beyond $x_{\text{Zn-Se}}$, corresponding to $x=0.92$ (refer to Fig. 2).

More generally the additional mode has the following characteristics. First it is a real (TO,LO) doublet since the LO-like mode emerges at significantly higher frequency than the TO-like one, as shown in Fig. 3. The two branches exhibit monotonic red shifts when x decreases. Concomitantly the LO-TO splitting reduces; the two branches converge around $400 \pm 3\text{ cm}^{-1}$ at $x \sim x_{\text{Be-Se}}$, which also appears in other data.¹¹ Besides regarding the intensity aspect, one crucial information is that the $\text{TO}_{\text{Be-Se}}^a$ mode grows at the cost of the nominal $\text{TO}_{\text{Be-Se}}$ mode when x increases. The balance between the intensities of latter two modes is equilibrated at $x \sim 0.5$. In fact, the $\text{TO}_{\text{Be-Se}}$ mode almost disappears at $x=0.67$ (refer to Fig. 2). This behavior is also atypical in multimode descriptions, it suggests that the additional and nominal BeSe-like TO modes are coupled in some way.

We notice that a weak extra mode persists for x below $x_{\text{Be-Se}}$ down to $x=0.09$ (see the inset in Fig. 3). However, this weak mode appears systematically at the same frequency in both geometries, i.e., $400 \pm 3\text{ cm}^{-1}$, independently of composition.

IV. DISCUSSION

Our aim now is to provide a framework for the quantitative discussion of the BeSe-like bi-modal behavior within the percolation regime. We have already underlined that the BeSe and ZnSe force constants differ by nearly a factor of 2. On this basis, we suggest that a pseudocontinuous hardlike submatrix builds up when x goes above $x_{\text{Be-Se}}$.

As a starting basis, it is necessary to summarize the way a host matrix, i.e., a continuum, in a ternary alloy acts upon a local given bond when the composition changes. As an example, we consider the nominal BeSe-like mode in ZnBeSe. At low Be content, owing to the lattice mismatch between ZnSe and BeSe, Be-Se bonds undergo a tensile strain due to the ZnSe-like matrix, which reduces the effective force constant. This gives rise to a local BeSe-like mode emerging at 445 cm^{-1} , i.e., below the optical band of BeSe, namely, $501\text{--}578\text{ cm}^{-1}$. As x increases the initial ZnSe-like host matrix turns BeSe-like so that the medium influence vanishes and the bulklike LO and TO frequencies are progressively recovered. These well-known bond-in-a-continuum frequency characteristics are typically accounted for by the phenomenological MREI model.¹³

A. Percolative context

As shown in Fig. 3 the TO-LO splitting of the additional mode obeys the MREI model for all but that a “rescaled” alloy is considered from $x_{\text{Be-Se}}$. The rescaling procedure consists first in a parametrization of the hardlike submatrix corresponding to a renormalized composition $y = (x - x_{\text{Be-Se}})(1 - x_{\text{Be-Se}})^{-1}$ varying from 0 to 1 for x between $x_{\text{Be-Se}}$ and 1. Second, the degenerated extra mode at $x \sim x_{\text{Be-Se}}$ located at $400 \pm 3\text{ cm}^{-1}$ is assigned as the true local mode of Be within latter submatrix. At last the $\text{LO}_{\text{Be-Se}}$ frequency is renormalized to $543 \pm 5\text{ cm}^{-1}$, as strongly suggested by the experimental data in Fig. 3. Besides the starting TO and LO frequencies for the Zn-Se bonds are taken as the nominal MREI values at $x = x_{\text{Be-Se}}$, namely, 214 and 251.5 cm^{-1} .¹² The frequencies of the $\text{TO}_{\text{Be-Se}}$ mode and the local mode of zinc in BeSe remain unchanged at 501 and 231 cm^{-1} , respectively. The resulting frequencies for the additional TO and LO modes are shown by solid lines in Fig. 3. A very good agreement with the experimental frequencies is seen.

As possible explanations for the atypical end frequencies required above we propose the following. Be-Se bonds “in excess” within the hardlike submatrix formed spontaneously above $x_{\text{Be-Se}}$ should undergo a larger tensile strain to match the surrounding lattice parameter than those resulting from a very low Be incorporation, dispersed within the softer ZnSe-like matrix. As a result the additional local BeSe-like mode ($x \sim x_{\text{Be-Se}}$) is shifted to lower frequency, i.e., $\sim 400\text{ cm}^{-1}$, than the nominal one ($x \sim 0$), at 445 cm^{-1} . Besides we sug-

gest that within the percolation range confinement effects due to intermixing of the two pseudocontinuous submatrices destroy long-range polarization effects. As a consequence, the propagating $\text{LO}_{\text{Be-Se}}$ mode within the hardlike submatrix would turn into a surface mode, as is indeed currently observed in confined systems, corresponding to a renormalized frequency within the optical band.²⁰ This is satisfactorily accounted for at each composition by taking the reduced LO frequency at $\sim 543 \text{ cm}^{-1}$ in end material BeSe for the MREI calculations. Microscopic approaches are needed to understand fully both frequency renormalizations.

To the best of our knowledge there are no vibrational data available in the literature in the Zn-dilute domain. Our data related to $x \sim 0.92$ provide, therefore, a check in at this limit. Above $x_{\text{Zn-Se}}$ the hardlike infinite cluster turns into a continuous medium and long-range polarization effects should be recovered. As a matter of fact the TO and LO BeSe-like frequencies calculated for $x = 0.92$ with the “rescaled” alloy by taking 578 cm^{-1} as the end frequency for the LO mode in BeSe are consistent with the data (not shown). In contrast, similar calculations performed with the MREI model corresponding to $\omega(\text{ZnSe:Be}) = 445 \text{ cm}^{-1}$ and $\omega(\text{LO}_{\text{Be-Se}}) = 578 \text{ cm}^{-1}$ bring unrealistically LO and TO frequencies on each side of the experimental ones (not shown).

The picture that emerges is that within the percolation range the alloy consists of a composite system made mainly of two interlaced but *separate* pseudocontinuous submatrices: a Be-rich region with relatively large stiffness coefficient, and a relatively soft Zn-rich region. Out of the percolation range the picture of a single matrix prevails. This is softlike in the Be-dilute limit and hardlike at the other extremity. The whole composition dependence of the BeSe-like phonon frequencies within ZnBeSe can be described in terms of a generalized version of the standard MREI model.

It is worth noticing that the above simple picture does not take into account that within the percolation range a distribution of finite-size hardlike and softlike clusters coexists with the two submatrices.²¹ Out of the percolation range the minor phase persists but is represented by the finite-size clusters only. In particular, below $x_{\text{Be-Se}}$ the persistence of the weak TO-LO degenerated contribution around 400 cm^{-1} (see the inset in Fig. 3) is interpreted as a “reminiscence” of the extra local mode of Be within the finite-size hardlike clusters. Further discussion of this mode goes beyond the scope of this work.

B. Coupling effect

We address now the key issue of the coupling between the nominal and additional BeSe-like optical modes. Within the percolation range both quasicontinuous submatrices are transparent to the exciting radiation, owing to the large gap of ZnBeSe alloys. In this condition, the LO and TO modes of the whole system should result mainly from the simple addition of the corresponding signals from each submatrix, weighted by their relative scattering volumes. Line shape analysis of the ZnSe- and BeSe-like modes is achieved within the Hon and Faust approach²² by taking linear dependency vs x (softlike continuum) and y (hardlike continuum)

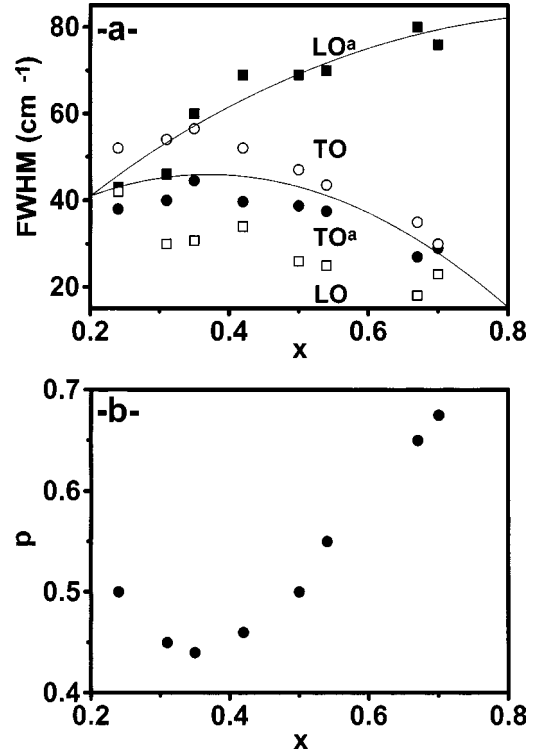


FIG. 4. Composition dependence for the full widths at half maximum of the optical modes (a) and for the volume fraction p of the hardlike submatrix (b). In part (a) thin solid lines are added as guidelines for the eyes.

for both the squares of the dynamical charges and the Faust-Henry coefficients, and by using equations of motion and polarization derived from the MREI model. The detailed procedure is reported elsewhere.¹⁸ If we neglect in a first approximation the persisting distributions of finite-size clusters that coexist with the two submatrices within the percolation range, the weighting factor is labeled p for the hardlike submatrix and $1 - p$ for the softlike one. It seems reasonable that $p \sim 1 - p \sim 0.5$ at $x = 0.5$. Satisfactory agreement with the observed intensities of the two BeSe-like TO modes at this composition requires the renormalization of the Faust-Henry coefficient related to bonding Be-Se within the hardlike submatrix. We find $C'_{\text{Be-Se}} = -0.6$, which differs by less than 15% from the nominal value, i.e., $C_{\text{Be-Se}} = -0.7$.¹⁸ Parameter p is then optimized at each composition from the observed TO intensity ratio. The damping coefficients of the optical BeSe-like modes used for the line shape calculations were obtained from the full width at half maximum of the experimental lines, reported in Fig. 4(a). One important information is that the treatment requires basically one parameter only (p) to account for the TO-like multimode behavior.

Alternatively, parameter p could also be derived at each composition from the ratio between the absolute intensity of the $\text{LO}_{\text{Be-Se}}$ mode and that of the corresponding theoretical line shape¹⁸ normalized to a layer thickness of $1 \mu\text{m}$. However, we have shown elsewhere that from $x \sim 0.5$ a near-interfacial disordered layer, with a Raman signal corresponding to a broad band at 250 cm^{-1} , is built up on the alloy side before the ordered alloy is grown up to the surface.²³ We

have also observed that this disordered layer enlarges when x increases. However, its real thickness is unknown at this stage, and the same holds true for the real thickness of the ordered alloy. This prevents any reliable treatment based on the absolute intensity of the $\text{LO}_{\text{Be-Se}}$ mode. For the presentation in Fig. 1 the theoretical line shapes are artificially normalized so as to obtain the best agreement between the experimental and calculated $\text{LO}_{\text{Be-Se}}$ modes.

The resulting LO and TO multimode line shapes agree rather well with the experimental curves, as shown in Figs. 1 and 2. No attention was awarded to the ZnSe-like TO modes since these are screened by the LA contributions. Concerning the LO symmetry, we notice that the additional ZnSe-like mode stays above the nominal one and accounts for the apparent blue shift of the experimental mode under x increase (refer to $x=0.62$ in Fig. 1).

However, there are significant discrepancies between the experimental and theoretical line shapes. First, we notice clear frequency shifts. Our present view is that these arise from a lattice parameter conflict between the coexisting hardlike (Be-rich) and softlike (Be-poor) clusters. Owing to the mechanical contrast latter conflict should not end up in homogenization, as in conventional ternary alloys, but should rather generate at any x internal strains within both submatrices. Second, it is remarkable that the calculated additional ZnSe- and BeSe-like LO mode systematically overestimates the corresponding experimental curve (refer to Fig. 1). Moreover, we notice from Fig. 4(a) that in contrast with the other optical modes the $\text{LO}_{\text{Be-Se}}^a$ mode becomes overdamped under x increase. The reasons for the overdamping and reduced strength of the additional LO mode remain unclear at this stage.

The evolution of parameter p vs x is shown in Fig. 4(b). Above $x_{\text{Be-Se}}$ up to $x \sim 0.4$, p is not an increasing function of x and remains unexpectedly large. This is attributed to the mixed character of the Raman signal at $\sim 400 \text{ cm}^{-1}$. As already mentioned this arises not only from the as-grown hardlike submatrix but also from a persisting distribution of isolated hardlike clusters. The Raman signal from the latter cannot be neglected close to $x_{\text{Be-Se}}$. As it does not come from a quasicontinuum, the MREI model is not relevant for its calculation, which brings an erroneous evolution of p vs x close to $x_{\text{Be-Se}}$. Under further Be incorporation the isolated clusters progressively coalesce and incorporate the hardlike submatrix that grows bigger, so that the picture of a single pseudocontinuous hardlike region should finally prevail. At this limit the MREI model should fully apply and the variation of p vs x should then provide information upon the growth of the hardlike infinite cluster under Be incorporation. Our $p(x)$ curve should, therefore, match asymptotically only future corresponding theoretical predictions.

We mention that the MREI approach was never considered before to account for multimode behaviors in Raman spectra of alloys. Either the statistical approach of Verleur and Baker²⁴ or the empirical one from Mintairov and Temkin²⁵ were systematically used. For a simplified comparison between the three methods, we restrict our discussion to the LO symmetry only.

The two usual approaches describe multimodes occurring at any composition, and attributed to different local atomic arrangements in an alloy otherwise considered as *homogeneous* at the macroscopic scale. In these conditions the LO line shapes are basically obtained from the imaginary part of a *single* dielectric function with multiple oscillators. With Mintairov's approach latter distribution is predetermined empirically at each composition and the problem then reduces to the determination of the characteristic phonon frequencies for each of the considered clusters. This is deduced from the phonon dispersion curves for the different microstructures calculated by using first-principles methods. The only free parameters are the oscillator strengths. These finally provide the relative population for each kind of cluster within the alloy. With Verleur and Baker's approach all possible clusters are *a priori* simultaneously considered. Their relative population within the alloy is fixed by the so-called probability f . All parameters are simultaneously left free, i.e., the phonon frequencies and oscillator strengths, both depending on unknown parameter f that is derived from a curve-fitting procedure at each composition.

In the present case the context is different since the observed multimode behavior occurs within the percolation range only, and exhibits an atypical coupling effect. Both characters are well accounted for by considering that the two pseudocontinua that coexist within the percolation range carry different mechanical properties. This macroscopic contrast would result directly from the unusually large contrast in the Zn-Se and Be-Se bond stiffness. The resulting picture for any alloy in the intermediate composition range is that of a composite system made mainly of two *distinct* infinite submatrices, each characterized by a *specific* dielectric function. Owing to the macroscopic character of these submatrices the dependences vs the composition of both the phonon frequencies and oscillator strengths in each dielectric function can be derived from the frequencies observed in the high-dilution limits according to the phenomenological MREI model. In a first approximation, the whole multimode behavior is determined by using a single free parameter corresponding to the relative volume fraction of each submatrix within the alloy.

C. LA extraordinary strength

One important remaining point is the atypical strength of the LA bands within the percolation range. This does not come from the near-interfacial disordered layer that forms from $x \sim 0.5$ since the intensity of the LA bands and the thickness of this layer have opposite variations when x increases. As a possible explanation, we propose that by getting into the percolation range mechanical disorder resulting from the intermixing of the soft and hardlike submatrices suddenly reduces the acoustic-phonon correlation length, and thereby enlarges $q \neq 0$ effects. Under further x increase the distribution of available wave vectors should give greater place to zone-edge modes, corresponding to the lowest correlation lengths, and become more and more narrow. As expected, maximum effect is observed at $x \sim 0.5$, corresponding to the closest intermixing. At this limit, we suggest that only very-near zone-edge modes should be allowed, with con-

comitant effect upon the strength of the Raman signals at the corresponding frequencies. As expected a symmetric evolution is observed at increasing values of x . The above approach remains basically valid for the allowed optical modes. We observe that most of the full widths at half maximum indeed go through a maximum at $x \sim 0.4$ [refer to Fig. 4(a)] corresponding approximately to the composition range associated with the largest mechanical disorder.

Out of the percolation range a single continuum prevails so that first the phonon correlation length becomes quasi-infinite, which drastically weakens the LA bands (refer to Figs. 1 and 2), and second, mechanical disorder vanishes that drives damping reduction and strength increase for the single BeSe-like lines (refer to $x = 0.92$). Below $x_{\text{Be-Se}}$ the full width at half maximum of the BeSe-like modes remains surprisingly large. This is attributed for a given branch of the (TO,LO) doublet to the disorder-induced activation of the other theoretically forbidden branch, both being quasidegenerated for small x values.^{9,12} The blue (red) asymmetry of the nominal TO (LO) mode below $x_{\text{Be-Se}}$ supports this assumption (refer to the inset in Fig. 3).

V. CONCLUSION

We observe an atypical multimode behavior in the Raman spectra of $\text{Zn}_{1-x}\text{Be}_x\text{Se}$, which belongs to the new attractive

class of ternary zinc-blende alloys involving highly contrasted bond stiffness. We use a simple percolative picture for its basic understanding. On the quantitative side our observations can be quantitatively explained in terms of a generalized version of the standard modified-random-element-isodisplacement model.

On the practical side this work provides direct vibrational evidence for a percolation behavior in a ternary semiconductor alloy. More precisely, we show that between the bond-percolation thresholds, i.e., $x \sim 0.2-0.8$, $\text{Zn}_{1-x}\text{Be}_x\text{Se}$ consists of two pseudocontinuous intermixed clusters with contrasted mechanical properties. It would be important to find out how the resulting mechanical disorder could affect the performance of related optoelectronic devices.

Possible occurrence of such effects should be investigated not only in other ternary II-VI Be chalcogenides but also in III-N-V alloys, such as $\text{GaN}_x\text{As}_{1-x}$ when reasonable nitrogen incorporation can be achieved.

ACKNOWLEDGMENT

The authors wish to thank warmly Professor Kailash Rustagi for useful discussion and critical reading of the manuscript.

*Author to whom correspondence should be addressed; Electronic address: pages@ipc.sciences.univ-metz.fr

¹L. Bellaïche, S.-H. Wei, and A. Zunger, *Phys. Rev. B* **54**, 17 568 (1996).

²P. H. Song and D. S. Kim, *Phys. Rev. B* **54**, R2288 (1996).

³P. Y. Yu, Z. Su, D. S. Kim, J. S. Kim, Y. S. Lim, Y. H. Yee, Y. H. Cho, J. S. Lee, J. H. Lee, J. S. Chang, B. D. Choe, D. H. Woo, E. J. Shin, D. Kim, K. Arya, and J. J. Song, *Phys. Rev. B* **54**, 10 742 (1996).

⁴D. S. Kim, H. S. Ko, Y. M. Kim, S. J. Rhee, S. C. Hohng, Y. H. Hee, W. S. Kim, J. C. Woo, H. J. Choi, J. Ihm, D. H. Woo, K. N. Kang, *Phys. Rev. B* **54**, 14 580 (1996).

⁵C. Vérié, in *Semiconductors Heteroepitaxy*, edited by B. Gil and R. L. Aulombard (World Scientific, Singapore, 1995), p. 73.

⁶R. M. Martin, *Phys. Rev. B* **1**, 4005 (1970).

⁷A. Waag, F. Fischer, K. Schull, T. Baron, H. J. Lugauer, Th. Litz, U. Zehnder, W. Ossau, T. Gerhard, M. Keim, G. Reuscher, and G. Landwehr, *Appl. Phys. Lett.* **70**, 280 (1997).

⁸F. Vigué, E. Tournié, and J. P. Faurie, *Appl. Phys. Lett.* **76**, 242 (2000).

⁹J. Geurts, V. Wagner, B. Weise, J. J. Liang, H. Lugauer, A. Waag, G. Landwehr, and R. Kruse, in *Proceedings of the 24th International Conference on the Physics of Semiconductors*, edited by D. Gershoni (World Scientific, Jerusalem, 1998), p. 1.

¹⁰F. Rozploch, F. Firszt, S. Legowski, H. Meczynska, J. Patyk, J. Szatkowski, and W. Paszkowic, in *Proceedings of the seventeenth International Conference on Raman spectroscopy*, edited

by S.-L. Zhang and B.-F. Zhu (John Wiley & Sons, Chichester, 2000), p. 550.

¹¹A. M. Mintairov, F. C. Peiris, S. Lee, U. Bindley, J. K. Furdyna, S. Raymond, J. L. Merz, V. G. Melehin, and K. Sadchikov, *Semiconductors* **33**, 1021 (1999).

¹²O. Pagès, M. Ajjoun, J. P. Laurenti, D. Bormann, C. Chauvet, E. Tournié, and J. P. Faurie, *Appl. Phys. Lett.* **77**, 519 (2000).

¹³I. F. Chang and S. S. Mitra, *Phys. Rev.* **172**, 924 (1968).

¹⁴C. X. Jin, Z. Ling, D. H. Wang, D. M. Huang, X. Y. Hou, X. Wang, *J. Appl. Phys.* **81**, 3465 (1997).

¹⁵J. Groenen, R. Carles, G. Landa, C. Guerret-Piécourt, C. Fontaine, M. Gendry, *Phys. Rev. B* **58**, 10 452 (1998).

¹⁶A. M. Mintairov, P. A. Blagnov, V. G. Melehin, N. N. Faleev, J. L. Merz, Y. Qiu, S. A. Nikishin, and H. Temkin, *Phys. Rev. B* **56**, 15 836 (1997).

¹⁷T. Ganguli and A. Ingale, *Phys. Rev. B* **60**, 11 618 (1999).

¹⁸O. Pagès, M. Ajjoun, D. Bormann, C. Chauvet, E. Tournié, and J. P. Faurie (unpublished).

¹⁹U. Fano, *Phys. Rev.* **124**, 1866 (1961).

²⁰R. Rupin, *J. Phys. C* **8**, 1969 (1975).

²¹D. Stauffer, *Introduction to Percolation Theory* (Taylor and Francis, London, 1985).

²²D. T. Hon and W. L. Faust, *Appl. Phys. Lett.* **1**, 241 (1973).

²³O. Pagès, M. Ajjoun, J. P. Laurenti, D. Bormann, C. Chauvet, E. Tournié, and J. P. Faurie, *Opt. Mater.* **17**, 323 (2001).

²⁴H. W. Verleur and A. S. Baker, *Phys. Rev.* **149**, 715 (1966).

²⁵A. M. Mintairov and H. Temkin, *Phys. Rev. B* **55**, 5117 (1997).